Available online at www.sciencedirect.com
SCIENCE DIRECT®
Journal of Luminescence 119–120 (2006) 204–208
JOURNAL OF LUMINESCENCE
www.elsevier.com/locate/jlumin

Nanoscale optical imaging of single-walled carbon nanotubes

A. Hartschuh[a,*], H. Qian[a], A.J. Meixner[a], N. Anderson[b], L. Novotny[b]

[a]*Institute of Physical and Theoretical Chemistry, University of Tuebingen, Tuebingen, Germany*
[b]*The Institute of Optics, University of Rochester, Rochester, NY 14627, USA*

Available online 31 January 2006

Abstract

In this contribution, we apply a microscopic technique that relies on the enhanced electric field near a sharp, laser-irradiated metal tip that acts as a highly confined light source. The tip is used for the local excitation of the optical response of single-walled carbon nanotubes (SWNT) deposited on glass. We demonstrate photoluminescence and Raman imaging of the same SWNTs with a spatial resolution of about 10 nm.

PACS: 61.46.+w; 07.79.−v; 78.30.Na; 78.67.Ch

Keywords: Single-walled carbon nanotubes; Near-field optical microscopy

1. Introduction

Nanotechnology and the exploration of the fascinating world of nanoscale materials require new tools with high spatial resolution. While atomic force microscopy (AFM) is a powerful tool to investigate the topography of nanoobjects and sample surfaces, it cannot provide information on their chemical composition and electronic properties. Optical techniques on the other hand directly probe electronic and vibrational transitions and are thus essential for the detection and analysis of individual nanoobjects such as single molecules, semiconductor quantum structures and biological macromolecules. Since diffraction limits the spatial resolution of conventional microscopy to about half the wavelength of light, new techniques have to be developed to extend optical spectroscopy to the nanometer regime. Sharply pointed optical fiber probes with sub-wavelength apertures are the most often used approach (see e.g. [1]). A number of disadvantages such as a very low throughput of light and a typical resolution of about 50–100 nm seem to restrict their widespread application. Optical antenna structures that rely on the local field enhancement effect represent a promising alternative (see e.g. [2–6]).

In this contribution, we present near-field optical imaging of single-walled carbon nanotubes

*Corresponding author. Fax: +49 7071 29 5490.
E-mail address: achim.hartschuh@uni-tuebingen.de (A. Hartschuh).

0022-2313/$ - see front matter © 2006 Elsevier B.V. All rights reserved.
doi:10.1016/j.jlumin.2005.12.031

(SWNTs) with a spatial resolution of about 10 nm. The method we use is based on the local field enhancement effect at a laser-illuminated metal tip that acts as a strongly confined excitation source.

SWNTs can be thought of as being formed by rolling up a two-dimensional graphite sheet into a seamless cylinder. They are typically between 0.5 and 2 nm in diameter, but several microns in length. Because of their unique mechanical and electrical properties, carbon nanotubes are considered for various technological applications, such as in integrated circuits, nanotube actuators and optoelectronic devices (see e.g. [7–9]). Both, photoluminescence (PL) and Raman spectroscopy combined with conventional microscopy have been used extensively to study the structural properties of SWNTs (see e.g. [10–13]). Recently, we demonstrated near-field Raman microscopy of individual SWNTs with high spatial resolution [4,14]. In this contribution, we show simultaneous near-field Raman and PL microscopy of SWNTs.

2. Experimental setup

The experimental setup is based on an inverted optical microscope with an x, y scan stage for raster scanning a transparent sample (see Fig. 1). A HeNe laser operating at 632.8 nm is used as excitation source. The laser beam is reflected by a dichroic beam splitter and focused by a high numerical aperture (NA) objective (1.25 NA) on the sample surface. A sharp gold tip is positioned in the focus of a radially polarized laser beam to achieve maximum field enhancement [15]. The tip is maintained above the sample surface at a distance of 1–2 nm by means of a sensitive shear-force feedback mechanism [16]. The optical signal is collected with the same objective, transmitted by the beam splitter and filtered by a notch filter to remove the fundamental laser light. The optical signal is detected either by a combination of a spectrograph and a cooled charged coupled device (CCD) or by two single-photon counting ava-

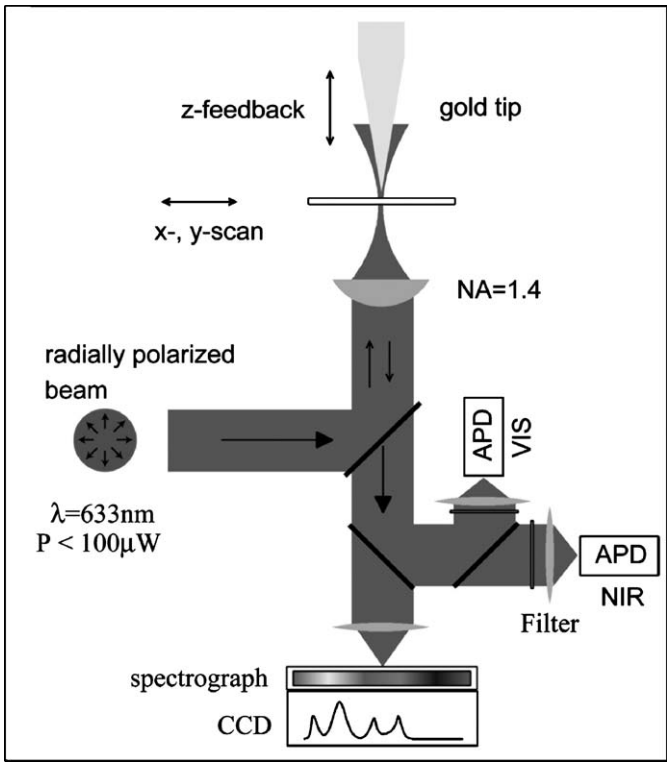

Fig. 1. Schematic of the experimental setup.

lanche photodiodes (APDs) after spectral filtering by narrow bandpass filters. A dichroic beam splitter is used to split the light into visible and IR-radiation so that two images of different spectral windows, typically a Raman and a PL-image, are obtained simultaneously. A near-field optical image is established by raster scanning the sample while recording the optical signals. Sharp gold tips are produced by electrochemical etching.

3. Near-field imaging of SWNTs

Fig. 2(b) shows the near-field Raman image of SWNTs on glass in a $1 \times 1\,\mu m^2$ scan area established by detecting the intensity of the Raman G-band upon laser excitation at 632.8 nm. In Fig. 2(a), the simultaneously acquired topography image of the sample is presented.

Cross-sections taken along the dashed lines in Fig. 2(a) and (b) are shown in (c) and (d) for the topographic and the optical image, respectively. The minimal width of the observed optical features is about 30 nm, far below the diffraction limit of light at this wavelength.

The optical and the topographic image are closely correlated and the SWNTs can be easily identified in both images. However, the intensity of the detected Raman signal does not scale with the topographical height of the observed tube features

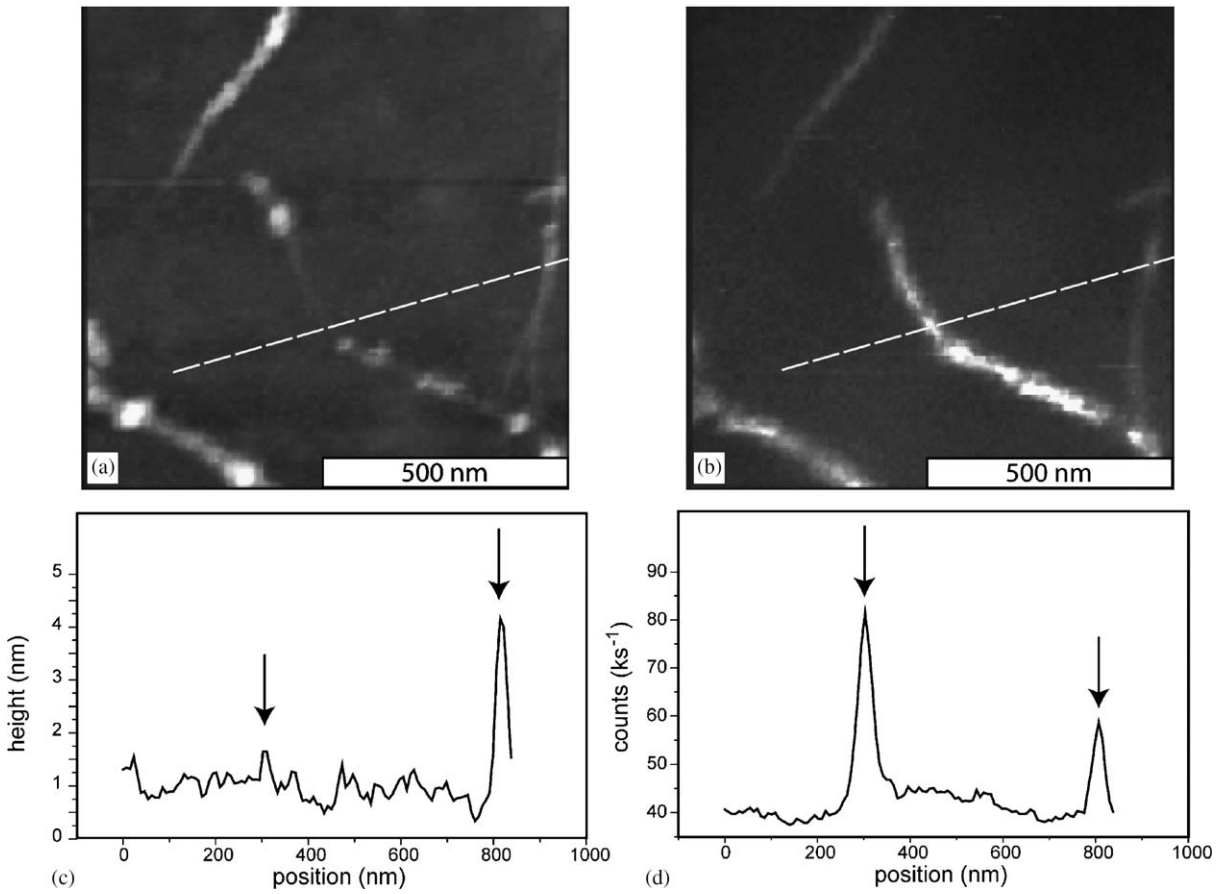

Fig. 2. Simultaneously acquired topography (a) and near-field Raman (b) image of SWNTs on glass. The near-field Raman image is established by integrating the intensity of the G-band of SWNTs at 700 nm corresponding to a Raman shift of about 1600 cm^{-1}. (c) and (d) show cross-sections taken along the dashed lines in (a) and (b) respectively. The arrows mark the positions of the most prominent Raman signals.

as can be seen by comparing the cross-sections in Fig. 2(c) and (d). While the strongest Raman signal occurs at a position of about 300 nm, as indicated by the arrow, the corresponding height of the tube at this position is less than 1 nm. The far higher topographical feature of about 5 nm at 820 nm, caused presumably by a tube bundle, renders a much weaker Raman signal. The observed differences between the optical and topographic image can be understood in terms of resonance Raman scattering. The Raman scattering strength of SWNT is known to be strongly dependent on the resonance Raman effect that reflects the energy difference between photon energies and the electronic energies of the tube [12]. The resonance Raman effect enhances the signal essentially and is the reason why even single tubes can be observed. Some of the tubes that are detected topographically in Fig. 2(a) will be non-resonant at 632.8 nm and therefore do not appear in the optical image in Fig. 2(b).

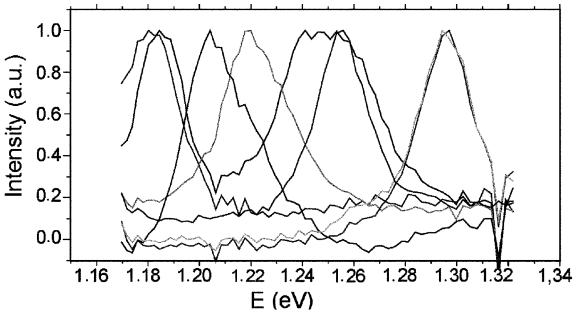

Fig. 3. Photoluminescence spectra of different SWNTs on glass detected for different sample positions.

In the literature, luminescence has only been reported for SWNTs freely suspended between pillars or for micelle encapsulated SWNTs [17,18]. Since the additional surfactant coating used in the latter case will significantly increase the tip–sample distance [18], a reduced signal enhancement is expected [4]. To avoid this, we tried to observe PL of SWNTs on glass. Surprisingly, the PL of tubes that were deposited directly on glass was found to be rather strong giving rise to broad emission spectra at different emission energies (see Fig. 3).

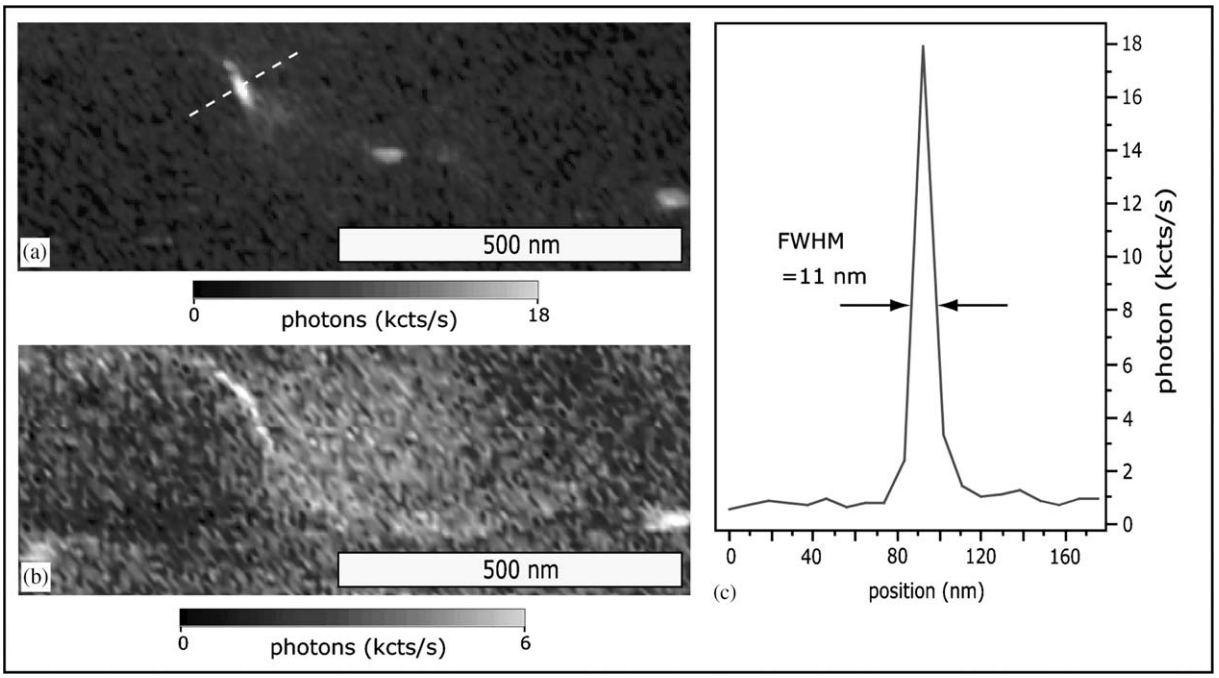

Fig. 4. Near-field Raman (a) and PL (b) image of SWNTs on glass. (c) cross-section along the dashed line in (a). The optical resolution achieved in the experiment is determined from the width (FWHM) of the optical signal to be about 10 nm.

A near-field PL image of SWNTs on glass is presented in Fig. 4(a) together with the simultaneously detected Raman image in (b). The PL image was formed by detecting the PL intensity in a 50 nm wide spectral window centered at 950 nm. Based on literature data, the PL presumably originates from an (8,3)-tube [10]. The width of the optical cross-section in Fig. 4(c) taken along the dashed line in Fig. 4(a) indicates a spatial resolution of about 10 nm. Remarkably, the PL signal occurs only within a very short segment of the tube whereas the Raman signal clearly has a larger extension. This localization of the PL could be caused either by local variations of the dielectric environment or by structural distortions and defects that are associated with non-radiative decay. In the future, we will investigate the role of structural defects in the excited state processes by studying correlated near-field Raman and PL spectra.

4. Summary

In this contribution, we applied tip-enhanced optical microscopy to study single-walled carbon nanotubes on glass with a spatial resolution of down to 10 nm. The spectroscopic information provided by this method allows us to distinguish between tube structures that are in resonance or off resonance with the incident photon energy thus giving an additional image contrast compared to AFM measurements. Near-field optical images revealed highly localized emission from tubes that will be subject of further investigations.

Acknowledgements

The authors thank Gregor Schulte for valuable experimental support. Financial support by the University of Siegen is gratefully acknowledged.

References

[1] E. Betzig, J.K. Trautman, Science 257 (1992) 189.
[2] E.J. Sánchez, L. Novotny, X.S. Xie, Phys. Rev. Lett. 82 (1999) 4014.
[3] N. Hayazawa, Y. Inouye, Z. Sekkat, S. Kawata, Chem. Phys. Lett. 335 (2001) 369.
[4] A. Hartschuh, E.J. Sánchez, X.S. Sunney, L. Novotny, Phys. Rev. Lett. 90 (2003) 095503.
[5] H.G. Frey, S. Witt, K. Felderer, R. Guckenberger, Phys. Rev. Lett. 93 (2004) 200801.
[6] J.N. Farahani, D.W. Pohl, H.-J. Eisler, B. Hecht, Phys. Rev. Lett. 95 (2005) 017402.
[7] R.H. Baughman, C. Cui, A. Zakhidov, Z. Iqbal, et al., Science 284 (1999) 1340.
[8] J.A. Misewich, R. Martel, Ph. Avouris, J.C. Tsang, et al., Science 300 (2003) 783.
[9] M. Freitag, J. Chen, J. Tersoff, J.C. Tsang, et al., Phys. Rev. Lett. 93 (2004) 076803.
[10] S.M. Bachilo, M.S. Strano, C. Kittrell, R.H. Hauge, et al., Science 298 (2002) 2361.
[11] A. Hartschuh, H.N. Pedrosa, L. Novotny, T.D. Krauss, et al., Science 301 (2003) 1354.
[12] A. Jorio, R. Saito, J.H. Hafner, C.M. Lieber, et al., Phys. Rev. Lett. 86 (2001) 1118.
[13] C. Jiang, J. Zhao, H.A. Therese, A. Mews, et al., J. Phys. Chem. B 107 (2003) 8742.
[14] N. Anderson, A. Hartschuh, S. Cronin, L. Novotny, J. Am. Chem. Soc. 127 (2005) 2533.
[15] L. Novotny, E.J. Sánchez, X.S. Xie, Ultramicroscopy 71 (1998) 21.
[16] K. Karrai, R.D. Grober, Appl. Phys. Lett. 66 (1995) 1842.
[17] J. Lefebvre, Y. Homma, P. Finnie, Phys. Rev. Lett. 90 (2003) 217401.
[18] M.J. O'Connell, S.M. Bachilo, C.B. Huffman, V.C. Moore, et al., Science 297 (1992) 593.